Magnetization measurements and computer simulations for the magnetic hysteresis losses of reentrant Ni$_{100-x}$Mn$_x$Pt and Ni-Mn alloys

Y. Öner and B. Aktaş

Hacettepe University, Department of Physics, Beytepe, Ankara, Turkey
(Received 5 February 1990)

We have carried out ac and dc magnetization measurements on Ni$_{74}$Mn$_{24}$Pt$_2$ alloy in the temperature range of 4.2–300 K. When 2 at. % platinum impurity atoms are substituted in place of nickel atoms, it has been observed that both the unidirectional and uniaxial anisotropies are significantly induced, while the freezing temperature (T_f) remains nearly unchanged within experimental uncertainty. In addition, the unusually large magnetic hysteresis losses (broadening loops) observed for this alloy have been attributed to the induced unidirectional anisotropy rotation and to the increase of the uniaxial anisotropy. In order to justify the assertion mentioned above, we have also introduced a simple model based on Kouvel's model by taking into account the elastic anisotropy rotation and the uniaxial anisotropy component.

INTRODUCTION

Magnetic and magnetotransport studies on Ni$_{100-x}$Mn$_x$ alloys (x lies between ~ 19 and 33 at. % Mn) are of interest in their own right because they include many new observations, such as resistivity minima,[1] double electron spin resonance (ESR) peaks,[2] asymmetric magnetoresistance,[3,4] unusual magnetic hysteresis losses,[5-7] etc., whose origins are still unknown and because they also shed some light on the origin of the unidirectional anisotropy appearing in many spin-glass (SG) and reentrantlike (RE) systems. It is well known that frustration in the spin system of the Ni-Mn alloys comes from the competition, on a local scale, between the ferromagnetic exchange coupling of Ni-Ni or Ni-Mn pairs and the antiferromagnetic coupling of Mn-Mn pairs. For the alloys of Mn concentration, $19 < x \leq 24$ at. %, the competition can become so strong that, as the temperature decreases from high to low temperatures, this system first passes through the paramagnetic (PM) state to the ferromagnetic (FM) state at a temperature T_c and then it evolves into the unstable state at the freezing temperature $T_f < T_c$ below which it has a spontaneous FM moment coexistent with the SG ordering. Thus, these alloys, which are called RE ferromagnets, show double magnetic phase transition. As the competition is further increased by adding still more Mn atoms, these alloys have no FM state at any temperature, but have a transition from the PM state to the SG state at the freezing temperature T_f, i.e., there is a multicritical point (MCP) in the magnetic phase diagram[8] of these alloys (x lies somewhere between 24 and 25 at. %) above which there is no long-range FM ordering.

In our previous papers,[9] we presented the results of a ferromagnetic resonance (FMR) study of these alloys in order to account for the behavior of the anisotropy field for either field-cooling (FC) or zero-field-cooling (ZFC) cases. We interpreted our results by introducing the elastic anisotropy rotations within the frame of the domain

anisotropy model.[10,11] According to this model, the magnetic state of the reentrant Ni-Mn at low temperature $(T < T_f)$ is characterized by frozen, random domains. Each domain has a unidirectional anisotropy field directed along its initial magnetization vector. This anisotropy in M versus H curves obtained for FC cases manifests itself as a shift towards negative fields.

The purpose of this paper is threefold: First, to get some further experimental evidence about our claim on
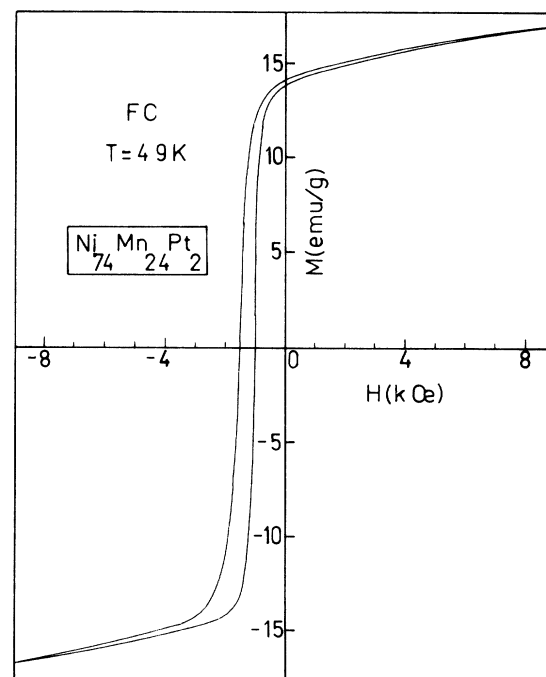

FIG. 1. The hysteresis loop for Ni$_{74}$Mn$_{24}$Pt$_2$ is plotted after cooling the sample in a field of 15 kOe down to 4.9 K (indicated by FC). Note that the shift of this loop is little more than 1 kOe.

the anisotropy rotation;[2,9,12] second, to investigate the effect of nonmagnetic impurities on the reentrant behavior of Ni-Mn alloys i.e., on the freezing temperature (T_f), the magnitude of the unidirectional anisotropy and also magnetic hysteresis losses; third, to extend the model of Kouvel[7,12] by introducing the elastic anisotropy rotations and the uniaxial anisotropy component[13] to interpret qualitatively the experimental results obtained on Ni-Mn-Pt ternary alloys. In fact, it was shown[14] that the unidirectional anisotropy is considerably enhanced by the addition of a few hundred ppm of Au or Pt nonmagnetic impurities to Cu-Mn SG alloys. Subsequently, P.M. Levy and A. Fert[15] have suggested a theory based on spin-orbit coupling including Dzyaloshinsky-Moriya (DM) type interaction and have shown that this anisotropy would be strongly enhanced due to the strong spin-orbit coupling.

EXPERIMENTAL RESULTS

The alloy specimens were prepared by melting together high purity Pt, Ni, and Mn, sealed into a quartz tube under Ar atmosphere ($\sim \frac{1}{3}$ atm), in an rf induction furnace, in which, after several hours of remelting, the specimen was quenched into water by breaking the quartz tube. Small disklike samples of 0.05 mm thickness and ~ 2.3 mm diameter were cut from rolling sheets. These sam-

ples were again encapsulated in a quartz tube (in vacuum) and were annealed for 3 h 900 °C and then water quenched.

Magnetization measurements were made with a homemade vibrating sample magnetometer whose sensitivity is about 10^{-5} emu. Magnetic field was provided by Electromagnet Model Varian up to 23 kG. Low-field ac susceptibility measurements were made using a mutual inductance method, where the sample could be removed from coils at each temperature and where in phase and in quadrature signals were simultaneously detected. The temperature was controlled by helium flow cryostat from 4.2 to 300 K.

Figure 1 shows the hysteresis of the magnetization versus the applied field on $Ni_{74}Mn_{24}Pt_2$ alloy, after cooling the sample in 15 kG magnetic field from the room temperature (~ 300 K) to about 5 K. This cooling field was assumed to be enough to reach nearly its saturation thermoremenant magnetization value. This M versus H curve shifts towards negative field. The amount of this shift is about 1 kG, which is twice that of $Ni_{76}Mn_{24}$ alloy prepared under the same conditions.[7]

Figure 2 shows the results of M versus hysteresis on Ni-Mn-Pt ternary alloy cooled in zero field to various fixed temperatures that are indicated on the figure. The most typical features of these curves are the following. First of all, the cycles are extremely large at low temperatures compared with the corresponding curves of Ni-Mn alloys at the concentration of 24 and 25 at. % Mn.[7,16] We have also plotted the magnetic losses as a function of the temperature (Fig. 3). The maximum value of the hysteresis losses is about $\sim 8 \times 10^5$ erg/cm^3, which is about twice that of disordered $Ni_{74.5}Mn_{24.5}$ (see Ref. 16, Fig. 5). It is interesting to see that the temperature T_m (~ 7 K) at which the losses passes through a maximum, is shifted to-
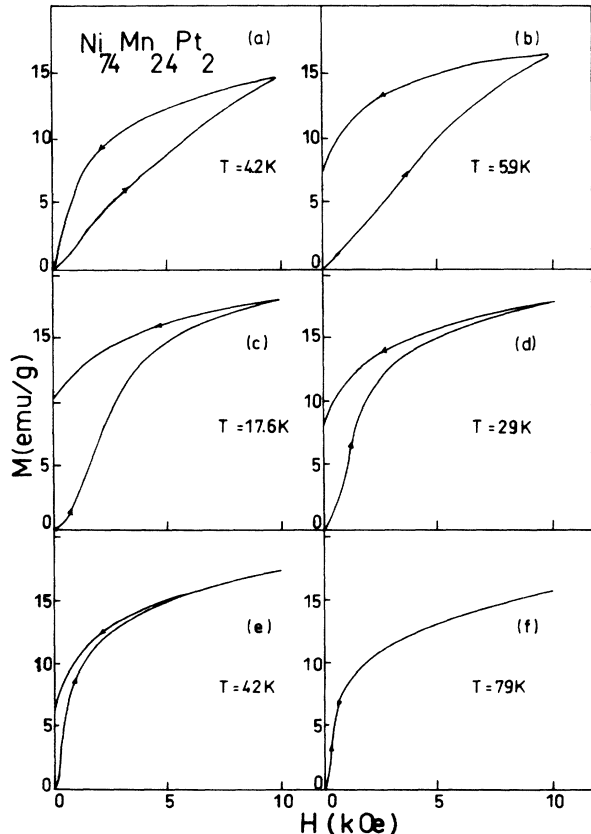

FIG. 2. A set of hysteresis loops for $Ni_{74}Mn_{24}Pt_2$ cooled in zero field (ZFC) down to the temperatures of measurements indicated in the figure.
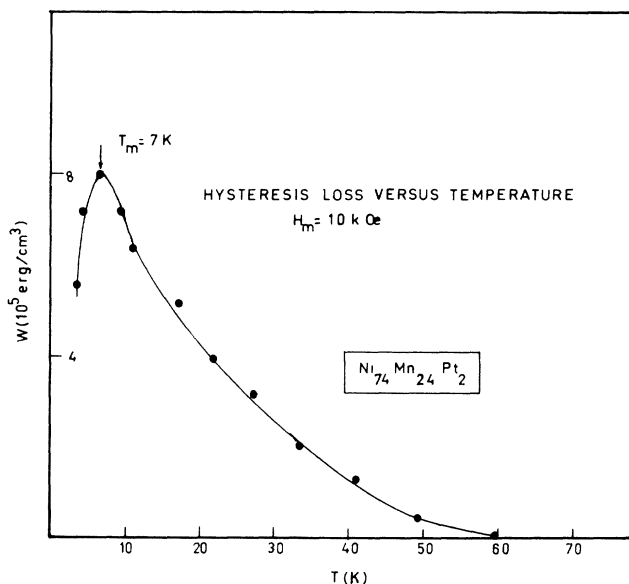

FIG. 3. Hysteresis loss for an external field cycled between ∓ 10 kOe vs temperature for $Ni_{74}Mn_{14}Pt_2$ cooled in zero field for each temperature indicated on figure.
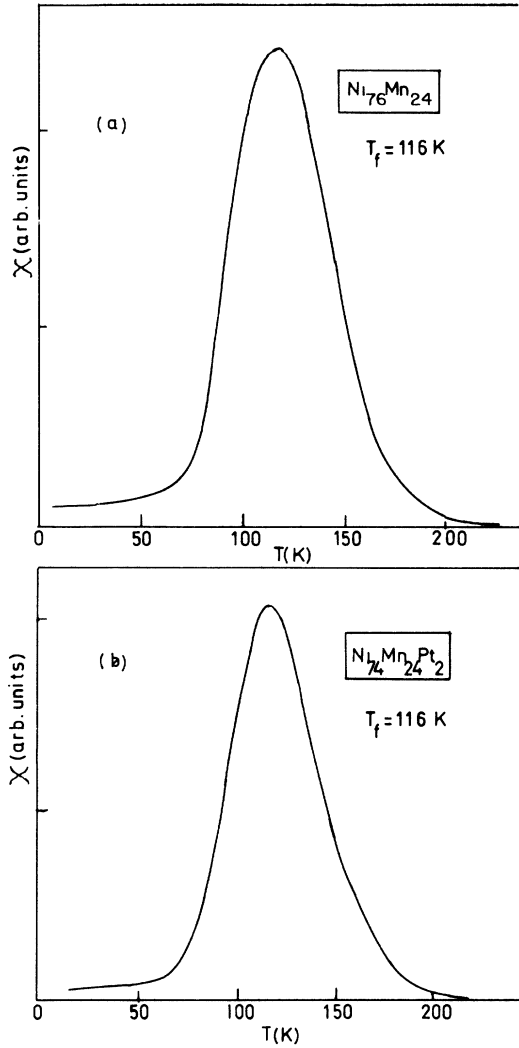
FIG. 4. Internal ac susceptibility at 88 Hz and 8 Oe rms vs temperature (a) for a disordered Ni-24 at %Mn sample (b) for a disordered ternary $Ni_{74}Mn_{24}Pt_2$. Note that the freezing temperatures of these alloys are nearly the same.
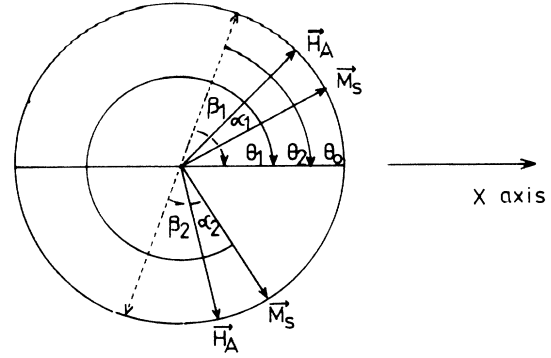

FIG. 5. Schematic vector representation of spin-glass domains with oppositely directed anisotropy fields; dashed vectors show the initial directions of the coupled domains.

wards the lower temperature compared with that of $Ni_{74.5}Mn_{24.5}$. This behavior can be understood if one assumes the anisotropy becomes considerably free to rotate. The second interesting feature of the curve concerns the evolution of the cycle with magnetic field. For ZFC cases, at low temperatures, magnetization initially increases smoothly up to a certain field value then it changes its slope and goes rather faster towards its saturation value. Subsequently, as the magnetic field is removed, first the magnetization decreases very slowly, then, decreases rather abruptly towards the origin. We can call this "winglike hysteresis."

Figure 4 shows the temperature dependence of the

zero-field susceptibility as measured for the $Ni_{74}Mn_{24}Pt_2$ and $Ni_{76}Mn_{24}$ alloys. As it can be seen, for both alloys, when the temperature was raised in an applied ac field of a few Oe (here ~8 Oe), the magnetization response remained small until the domain (or aggregate of spins) *melted* at about 50 K and then magnetization increased rather abruptly and passed through a maximum at about 116 K. The freezing temperatures were the same for both of these two alloys. This suggests that the freezing process comes from the antiferromagnetic coupling between Mn atoms. But it requires further study to reply to the question of whether the Néel temperature of Mn plays important role in the freezing process.

MODEL AND DISCUSSION

The present model for Ni-Mn is similar to the model of Kouvel[7,12] with the only difference being that it includes both the unidirectional anisotropy rotation and the uniaxial component of the anisotropy. Considering the suggestion by Kouvel mentioned in their recent papers,[7,12] we also assume that, for ZFC cases, *similar but smaller domains* are distributed at random, and interactions between the domains oppositely directed are predominant. We also believe that such a simple situation is likely to provide the best test of the model.

We will first consider a coupled domain with oppositely directed anisotropy field whose anisotropy axes initially make an arbitrary angles θ_0 and $\theta_0 + \pi$ with the applied field direction ($+x$ axis) for each antiparallel domain. Figure 5 shows the vector diagram of the unidirectional anisotropy, H_A and the saturation magnitazition, M_s for a given external applied field. When the field is applied along the x axis, it will cause both M_s and H_A to rotate towards the direction of the applied field from their initial directions. Referring to Fig. 5, the energy of this system will be the sum of anisotropy and magnetic potential energies, i.e.,

$$E = W_1 |-M_s H \cos\theta_1 - M_s H_A \cos\alpha_1 + K_1\cos\beta_1 + K_2\sin^2(\theta_0 - \theta_1)|$$
$$+ W_2 |-M_s H \cos\theta_2 - M_s H_A \cos\alpha_2 + K_1\cos\beta_2 + K_2\sin^2(\theta_0 + \pi - \theta_2)| - H_E M_s \cos(\theta_2 - \theta_1) ,$$

where

$$\alpha_1 = \theta_0 - (\theta_1 + \beta_1) \quad \text{and} \quad \alpha_2 = \pi + \theta_0 - (\theta_2 + \beta_2) \ .$$

Here, α_1 denotes the angle between $\mathbf{M}_s$ and $\mathbf{H}_A$, θ_1 shows the angle between $\mathbf{H}$ and $\mathbf{M}_s$ and β_1 is the angle between $\mathbf{H}_A$ and its initial direction for the domain oriented favorably to the applied field; α_2, θ_2, and β_2 are corresponding angles for the other domain. The terms are described as follows.

(i) W_1 and W_2 are the weight factors which are equal to one for ZFC cases. For FC cases, their values will be given in the following. (ii) The terms with K_2 show the uniaxial component of the anisotropy energy as suggested by Hippert and Alloul.[13] (iii) The anisotropy rotation and its unidirectional character are given by the terms K_1 whose magnitude gives a criterion about the freedom of the unidirectional anisotropy. The larger K_1, the more rigid $\mathbf{H}_A$. (iv) $-M_s H \cos\theta_{1,2}$ and $-M_s \cos\alpha_{1,2}$ terms are the magnetic potential energies with respect to the applied field H and the anisotropy field $\mathbf{H}_A$, respectively. (v) The $-H_E M_s \cos(\theta_2 - \theta_1)$ term represent the mutual magnetostatic energy density of domain sets.

This term may be interpreted physically as follows. It is well known that when a magnetized crystal is heated above the Curie point and cooled again, it becomes demagnetized, giving rise to a number small domains, in order to reduce its demagnetizing field and the associated magnetostatic energy. In this study, we assume that our specimens contain a number oppositely magnetized domain sets in zero-field-cooling cases. When a field is applied, the domain as a whole will rotate rigidly and elastically against the relatively weak DM type forces that produce the unidirectional domain anisotropy, because of the strong coupling (e.g., by Heisenberg-type interaction) between the frustrated spins in each domain. The flux lines will therefore be disturbed due to domain rotations. Thus the adjacent domains interact magnetostatically with each other during rotations so that the magnetostatic energy becomes a minimum. In other words, this magnetostatic interaction may be regarded as a force which tends to keep neighboring domains antiparallel to one another. It should be noted that the contribution of this term to the total energy density depends not only on the relative orientations of the adjacent domains, but also on their volumes. It is relatively small for the Ni-Mn alloys whose Mn concentration is smaller than 24.5 at. % (i.e., below the multicritical point).

By minimizing E with respect to $\theta_1, \theta_2, \beta_1, \beta_2$, we can obtain the stable position for M_s with the applied field. Here H_A, M_s, K_1, K_2, and H_E are domain model parameters, while $\theta_1, \theta_2, \beta_1, \beta_2$ are variables. The simultaneous solutions for these variables at different H have been obtained by using computer program. The magnetization of the coupled domains along the applied field will be given as

$$M_a(\theta_0, H) = \tfrac{1}{2} M_s (\cos\theta_1 + \cos\theta_2) \ ,$$

which requires that M_s must be known separately. Averaging over all possible angles of θ_0, we can deter-mine the magnetization of the whole system, from

$$M(H) = \int_0^1 M_a(x, H) dx \ ,$$

where $x = \cos\theta_0$ and, from symmetry, the integration can be restricted to positive values of x as shown in the integration.

Now, we will determine the weight factors for a given cooling field, H_c. When the sample is cooled in a field from high temperatures $T > T_f$ to low temperatures, all domain will be frozen, keeping its domain configuration at $T = T_f$. This assumption was accepted for simplicity. In addition, it may be assumed that the domains are in thermal equilibrium at $T \geq T_f$, so that their probability distribution may be described by the Boltzmann distribution law. Thus, if the probability density in the absence of a field is $p(0)$, then when a field H is present, it becomes

$$p(H) = p(0)\exp\left[-\frac{U}{k_B T} \right] \ ,$$

where U is the potential energy of the domain in the field. If the domain has a moment $v\mathbf{M}_s$, the potential energy is $-(\mathbf{M}_s \cdot \mathbf{H})v$, where v is the smallest volume of a domain, so that

$$p(H, \theta) = p(0)\exp\left| \frac{M_s v}{k T_f} H_c \cos\theta_0 \right|$$

is obtained.

This, of course, neglects interaction between domains. The other way to interpret this probability distribution is that, in an applied field, the volume of domains which are favorably oriented by a Boltzmann factor of

$$\exp[(v H_c M_s / k T_f)\cos\theta_0]$$

at the expense of the other unfavorably oriented by a factor of

$$\exp\left| -\left[\frac{v H_c M_s}{k T_f} \right]\cos\theta_0 \right|$$

at $T \geq T_f$. In order to keep spherical distribution of domains in specimen, it is also assumed that the cooling field, H_c is so weak that the maximum volume of domains cannot exceed $\sin\theta_0 d\theta_0$ in an element of solid angle $d\Omega_0$. However, we have restricted ourselves to the case in which the maximum value of $H_{0c} = v H_c M_s / k T_f$ has been taken to be two in order to make sure that keeping the spherical distribution of domain still persists. So, the weight factors W_1 and W_2 become $\exp|H_{0c}\cos\theta_0|$ and $\exp|-H_{0c}\cos\theta_0|$, respectively. It is now easy to show that the magnetization of the domain set can be given as

$$M_c(\theta_0, H) = \left[\frac{e^{H_{0c}\cos\theta_0}}{e^{H_{0c}\cos\theta_0} + e^{-H_0\cos\theta_0}}\right] M_s\cos\theta_1$$

$$+ \left[\frac{e^{-H_{0c}\cos\theta_0}}{e^{H_{0c}\cos\theta_0} + e^{-H_{0c}\cos\theta_0}}\right] M_s\cos\theta_2 \ ,$$

where H_{0c} is the cooling field parameter. Then by averaging over all domain sets, keeping a random distribution, we can determine the magnetization of the whole system for FC cases as

$$M_c(H) = \int_0^1 M_c(\theta_0, H)\sin\theta_0 d\theta_0 \ .$$

All magnetization values have been normalized to give M_s for the infinite value of the applied field.

Thus, we will be able to give some calculated M versus H curves with various K_1, K_2, and H_E values for both ZFC and FC cases. Figure 6(a) shows the ZFC curve with $K_1 = 300$, $K_2 = 70$, and $H_E = -10$. This curve is quite similar to the experimental curves obtained on some reentrant alloys.[7,17] As can be seen, the curve progresses linearly up to the certain critical value of the applied field where the magnetization is reversible and then increases abruptly, but in a nonlinear fashion, towards its saturation value, M_s and it also gives rise to a hysteresis down
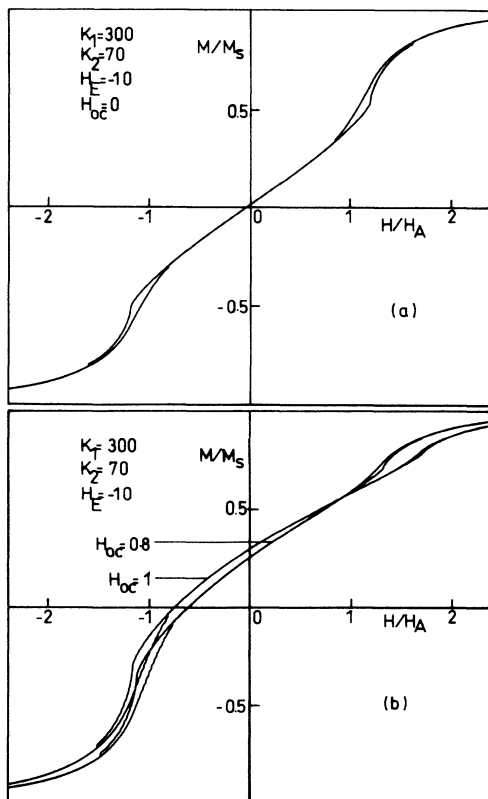
to the critical value of the applied field that were already mentioned. Figure 6(b) shows the simulated curve with the same values of K_1, K_2, and H_E as that of Fig. 6(a) but for the various cooling field factors indicated on the figure. As stated by Kouvel "*a smaller antiferromagnetic coupling is needed for the fit to the experimental curves of Ni-Mn system when the SG domains are arranged in aggregates.*" The antiferromagnetic coupling that was pointed out in the preceding statement of Kouvel corresponds to the magnetostatic interaction we mentioned in our previous discussion. This term, however, is not very important for the alloys below the multicritical point (24 at. % Mn). It is also remarkable to note that K_1 and K_2 are responsible for hysteresis losses, whereas the value of H_E only changes the initial slope of the ZFC curves i.e., the larger negative H_E, the smaller initial slope and its increasing value moves the inflection point to higher field.
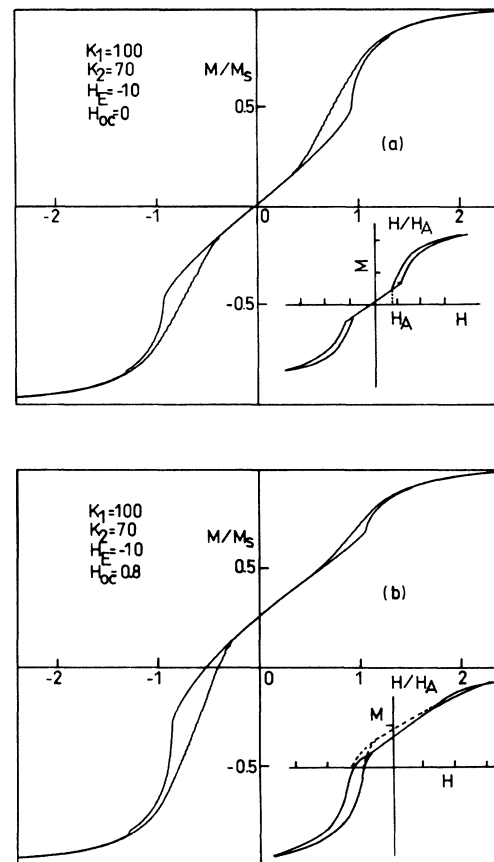

FIG. 7. Model curves to simulate the experimental curves of $Ni_{79}Mn_{21}$ alloy (a) for ZFC case (b) for FC case. The estimated values of the parameters are given in the figure. Inset in (a) shows the complete hysteresis loop for $Ni_{79}Mn_{21}$ alloy at 1.5 K after cooling the sample in zero field. Inset in (b) shows two hysteresis loops for $Ni_{79}Mn_{21}$ at 1.5 K: dashed curve was recorded after cooling in a steady field of 100 G from 25 to 1.5 K; full curve was recorded after cooling in $H = 0$ but in the presence of a remanent magnetization prepared at 25 K (these curves were taken from Ref. 18, Figs. 1 and 2). Note the similarity between the model curves and the corresponding experimental ones.

FIG. 6. Normalized total magnetization vs H/H_A, where H_A is the unidirectional anisotropy, (a) for ZFC cases (b) for FC cases. Note these curves reflect the nature of the reentrant spin-glasslike state of Ni-Mn alloys as described in the text.

Taking appropriate values of K_1, K_2, and H_E, one can thus get the simulated curve which fits better to the experimental one. If we let the anisotropy rotate more freely (i.e., smaller value of K_1), hysteresis losses increases and reversible part of the curves decreases. Also, the hysteresis losses increase with increasing K_2. For example, Fig. 7(a) shows the ZFC curve with the same parameters as those of Fig. 6(a), except the case with $K_1 = 100$. The inset in Fig. 7(a) shows the experimental ZFC curve for $Ni_{79}Mn_{21}$ alloy taken from the paper of Senoussi.[18] Figure 7(b) shows the FC curve for $H_{0c} = 0.8$. Inset in this figure shows the experimental FC curve for $Ni_{79}Mn_{21}$ alloy. The similarities between the experimental and simulated curves are very impressive. The experimental FC hysteresis loop for this alloy at 1.5 K had been recorded after cooling in a steady field of 100 G from 25 to 1.5 K. The most important part of this model concerning its validity, which encourages us, is that for intermediate field cooling conditions, the simulated curves give such a good similarity to the experimental curves obtained on Ni-Mn reentrant alloys.[17,18] This picture gives another support on the claim that *the anisotropy field is principally determined by the spatial distribution of the spontaneous magnetization during cooling field rather than by the cooling field eventually present* as reported by
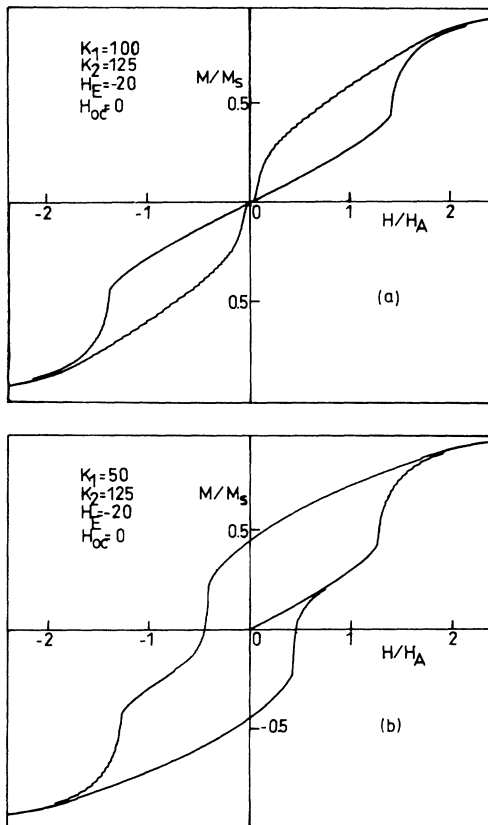
Senoussi in his paper.

We would like to present some curves simulated to the ZFC curves of the $Ni_{79}Mn_{24}Pt_2$ alloy at low temperatures. It is clear that Figs. 8(a) and 8(b) and Figs. 2(a) and 2(b) are quite similar. Such a result suggests that, to a first approximation, the unidirectional anisotropy becomes more free to rotate and both the unidirectional and uniaxial anisotropies are enhanced by adding nonmagnetic Pt impurity atoms. Allowing the anisotropy a little more room to rotate gives rise to a remanent [see Fig. 8(b)], which is called isothermal remanent anisotropy (IRM), being consistent with the corresponding experimental curves [see Figs. 2(b) and 2(c)].

As for Ni-Mn alloys whose Mn concentration is higher than 24 at. % the contribution of H_E is no longer small. Kouvel has recently pointed out that the average effect of the antiferromagnetic exchange field between neighboring domains pronounce itself more drastically in this regime. However, in connection with this, we propose the following. It is obvious that for the smaller domains, the contribution to the energy density from domain-domain magnetic interaction that are based on magnetostatics will be relatively important. The inset on Fig. 9 shows the magnetization versus the applied field of $Ni_{75}Mn_{25}$ for various cooling fields. It can be seen that as the cooling field decreases, the corresponding hysteresis curve shifts towards more negative field region i.e., the cooling field for the curve at left most is the smallest one. In Fig. 9, we have plotted the curves for the three different values of H_{0c} simulated to those in the inset on the same figure. As far as the displacement are concerned, the model gives quite adequate results. But the hysteresis losses were found to be different from those of the experimental curves. This small difference leads us to think over more about the validity of the domain anisotropy model on the Ni-Mn alloys in SG regime.
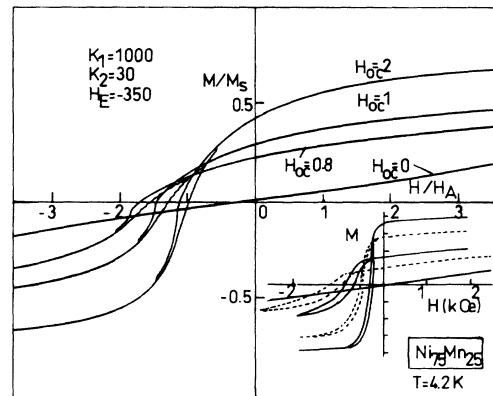

FIG. 8. (a) Model curve to simulate the experimental ZFC curves of $Ni_{74}Mn_{24}Pt_2$ alloy at low temperatures. (b) Model curve to simulate the experimental ZFC curves with IRM of $Ni_{74}Mn_{24}Pt_2$ alloy.

FIG. 9. Calculated magnetic hysteresis loops for different cooling-field parameter (H_{0c}) to simulate the curves of Ni-Mn alloys in spin-glass regime. Inset shows the magnetic hysteresis loops for $Ni_{75}Mn_{25}$ alloy after cooling to 4.2 K in different fields (it was taken from Ref. 7, Fig. 7). Note the similarity between the calculated curves and the corresponding experimental ones. The curves are for the cooling fields of 0, 200, 500, 2000, 10 000 Oe, respectively (bottom to top on the right).

CONCLUSION

The most important result of this paper concerns the influence of Pt impurities on the magnetic properties of the reentrant spin glass $Ni_{1-x}Mn_x$ systems. From this study it is found that Pt has no detectable effect on T_f. As it is found, from the study[19,20] on Cu-Mn and Cu-Mn doped nonmagnetic impurities, it can be seen that the influence of Au impurities on T_f is rather smaller than that of the other impurities. This behavior can be attributed to the fact that Pt and Au are isoelectronic with Ni and Cu, respectively. On the other hand, adding 2% of at. Pt leads to a large broadening of the hysteresis cycle (and a strong increase of the associated irreversibilities) and an enhancement of the unidirectional anisotropy without any change of the ferromagnetic spin glass transition temperature. This is a very interesting result which confirms that the $M(H)$ curve is controlled principally by DM anisotropy and domain rearrangements.

We also give full support to the experimental study carried out by Senoussi in order to understand how the anisotropy fields correlate with the spatial distribution of the spontaneous magnetization during cooling in its own internal field.

In conclusion, the results of this model account quite well for most of the gross feature of the unusual magnetic hysteresis loops of the Ni-Mn system for both ZFC and FC cases. But, it does not give much satisfactory results for SG regime. In short, the model used here seems, however, to be fairly good to a first approximation.

[1]S. Senoussi and Y. Öner, Phys. Rev. B 28, 455 (1983).

[2]Y. Öner, B. Aktaş, F. Apaydin, and E. A. Harris, Phys. Rev. B 37, 5866 (1988).

[3]S. Senoussi and Y. Öner, J. Appl. Phys. 55, 1472 (1984).

[4]J. Schaf and P. Pureur, J. Magn. Magn. Mater. 68, 358 (1987).

[5]S. Senoussi, J. Phys. 45, 315 (1984).

[6]W. Abdul-Razzaq and J. S. Kouvel, J. Appl. Phys. 55, 1623 (1984).

[7]J. S. Kouvel, W. Abdul-Razzaq, and Kh. Zig, Phys. Rev. B 35, 1768 (1987), and references therein.

[8]W. Abdul-Razzaq and J. S. Kouvel, Phys. Rev. B 35, 1764 (1987).

[9]B. Aktaş, Y. Öner, and E. A. Harris, Phys. Rev. B 39, 528 (1989).

[10]S. Senoussi and Y. Öner, J. Magn. Magn. Mater. 40, 12 (1983).

[11]J. S. Kouvel and W. Abdul-Razzaq, J. Magn. Magn. Mater. 53, 139 (1985).

[12]Y. Öner, T. Firat, İ. Ercan, and B. Aktaş, J. Magn. Magn. Mater. 72, 237 (1987).

[13]H. Alloul and F. Hippert, J. Phys. (Paris) Lett. 41, L201 (1980).

[14]J. J. Prejean, M. Toliclere, and P. Monod, J. Phys. (Paris) 41, 427 (1980).

[15]P. M. Levy, C. Morgan-Pond, and A. Fert, J. Appl. Phys. 53, 2168 (1982), and references therein.

[16]R. B. Goldfarb and C. E. Patton, Phys. Rev. B 24, 1360 (1981).

[17]W. Abdul-Razzaq and J. S. Kouvel, J. Appl. Phys. 57, 3467 (1985).

[18]S. Senoussi, Phys. Rev. Lett. 51, 2218 (1983).

[19]D. C. Vier and S. Schultz, Phys. Rev. Lett. 59, 150 (1985).

[20]A. Fert, N. de Courtenay, and H. Bouchiat, J. Phys. (Paris) 49, 1173 (1988).